Corrections

EVOLUTION. For the article "Clonal population structure and genetic diversity of *Candida albicans* in AIDS patients from Abidjan (Côte d'Ivoire)," by François Nébavi, Francisco J. Ayala, François Renaud, Sébastien Bertout, Serge Eholié, Koné Moussa, Michèle Mallié, and Thierry de Meeûs, which appeared in issue 10, March 7, 2006, of *Proc. Natl. Acad. Sci. USA* (**103,** 3663–3668; first published February 24, 2006; 10.1073/pnas.0511328103), the affiliation symbols for Thierry de Meeûs appeared incorrectly in the author line. The online version has been corrected. The corrected author line and the original affiliations and footnotes appear below.

François Nébavi*, Francisco J. Ayala†‡, François Renaud§, Sébastien Bertout*, Serge Eholié¶, Koné Moussa‖, Michèle Mallié*, and Thierry de Meeûs§**

*Laboratoire de Parasitologie et Mycologie Médicale, EA 2413, Faculté de Pharmacie, 34060 Montpellier Cedex 1, France; §Génétique et Evolution des Maladies Infectieuses, Equipe Evolution des Systèmes Symbiotiques, Unité Mixte de Recherche 2724, Institute de Recherche pour le Développement, Centre National de la Recherche Scientifique, BP 64501, 34394 Montpellier Cedex 5, France; ¶Service des Maladies Infectieuses et Tropicales, Centre Hospitalier Universitaire de Treichville, 01 BP V 3 Abidjan, Côte d'Ivoire; ‖Laboratoire de Parasitologie Mycologie, Institut Pasteur de Côte d'Ivoire, BP V 116 Abidjan, Côte d'Ivoire; and †Department of Ecology and Evolutionary Biology, University of California, Irvine, CA 92697

‡To whom correspondence may be addressed at: Department of Ecology and Evolutionary Biology, University of California, 321 Steinhaus Hall, Irvine, CA 92697-2525. E-mail: fjayala@uci.edu.

**To whom correspondence may be addressed. E-mail: demeeus@mpl.ird.fr.

www.pnas.org/cgi/doi/10.1073/pnas.0601704103

IMMUNOLOGY. For the article "First molecular and biochemical analysis of *in vivo* affinity maturation in an ectothermic vertebrate," by Helen Dooley, Robyn L. Stanfield, Rebecca A. Brady, and Martin F. Flajnik, which appeared in issue 6, February 7, 2006, of *Proc. Natl. Acad. Sci. USA* (**103,** 1846–1851; first published January 30, 2006; 10.1073/pnas.0508341103), the authors note that on page 1849, the last sentence of the first paragraph, left column, "The 10-fold increase in affinity observed for PBLA8 when compared with ancestral is mainly a consequence of a slower dissociation rate (≈5-fold slower than ancestral), whereas association rate is only fractionally improved (≈2-fold)," should read: "The 10-fold increase in affinity observed for PBLA8 when compared with ancestral is a consequence of its much slower dissociation rate (≈20-fold slower than ancestral), whereas its association rate is actually fractionally slower (≈2-fold)." This error does not affect the conclusions of the article.

www.pnas.org/cgi/doi/10.1073/pnas.0601790103

NEUROSCIENCE. For the article "Anxiolytic- and antidepressant-like profiles of the galanin-3 receptor (Gal_3) antagonists SNAP 37889 and SNAP 398299," by Chad J. Swanson, Thomas P. Blackburn, Xuexiang Zhang, Kang Zheng, Zhi-Qing David Xu, Tomas Hökfelt, Toni D. Wolinsky, Michael J. Konkel, Heidi Chen, Huailing Zhong, Mary W. Walker, Douglas A. Craig, Christophe P. G. Gerald, and Theresa A. Branchek, which appeared in issue 48, November 29, 2005, of *Proc. Natl. Acad. Sci. USA* (**102,** 17489–17494; first published November 15, 2005; 10.1073/pnas.0508970102), it should have been noted that Tomas Hökfelt is a consultant to Lundbeck Research USA, Inc. In addition, the authors note the following: "In Fig. 1, there are two concentrations on the graph where two distinct data sets representing different concentrations were included at a single concentration [pGal (log M) = −9 and −10, respectively]. In fact, one set of data at each of these concentrations was actually gathered at half-log concentrations (−7.5 and −8.5)." The corrected figure and its corrected legend appear below.

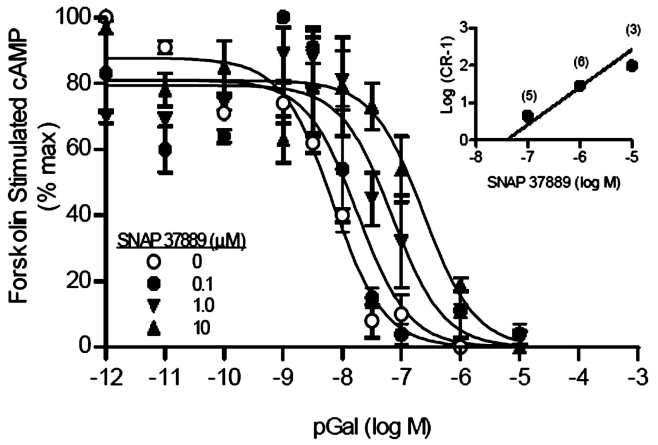

Fig. 1. SNAP 37889 is a competitive antagonist at the Gal_3 receptor. SNAP 37889 produced dose-related shifts in the concentration–effect curve to galanin in the adenylyl cyclase assay (representative experiment, $n = 4$). (*Inset*) Schild regression of the mean EC_{50} values affords a slope of 0.69 ± 0.12 and, when constrained to a unit slope, a pK_b value of 7.42 (K_b = 38 nM; n = 3–6 as shown on graph).

www.pnas.org/cgi/doi/10.1073/pnas.0601563103

First molecular and biochemical analysis of *in vivo* affinity maturation in an ectothermic vertebrate

Helen Dooley*†, Robyn L. Stanfield‡, Rebecca A. Brady*, and Martin F. Flajnik*§

*Department of Microbiology and Immunology, University of Maryland School of Medicine, 655 West Baltimore Street, Baltimore, MD 21201; §National Aquarium in Baltimore, 501 East Pratt Street, Baltimore, MD 21202; and ‡Department of Molecular Biology, The Scripps Research Institute, 10550 North Torrey Pines Road, La Jolla, CA 92037

Edited by Max D. Cooper, University of Alabama, Birmingham, AL, and approved December 14, 2005 (received for review September 23, 2005)

The cartilaginous fish are the oldest phylogenetic group in which Igs have been found. Sharks produce a unique Ig isotype, IgNAR, a heavy-chain homodimer that does not associate with light chains. Instead, the variable (V) regions of IgNAR bind antigen as soluble single domains. Our group has shown that IgNAR plays an integral part in the humoral response of nurse sharks (*Ginglymostoma cirratum*) upon antigen challenge. Here, we generated phage-displayed libraries of IgNAR V regions from an immunized animal and found a family of clones derived from the same rearrangement event but differentially mutated during expansion. Because of the cluster organization of shark Ig genes and the paucicopy nature of IgNAR, we were able to construct the putative ancestor of this family. By studying mutations in the context of clone affinities, we found evidence that affinity maturation occurs for this isotype. Subsequently, we were able to identify mutations important in the affinity improvement of this family. Because the family clones were all obtained after immunization, they provide insight into the *in vivo* maturation mechanisms, in general, and for single-domain antibody fragments.

immunoglobulin | somatic hypermutation

The canonical view of humoral immunity in warm-blooded vertebrates is that, after antigen challenge, serum antibodies improve in specificity and affinity with time (1). Low-affinity antibodies produced early in the response are essentially germ-line-encoded, whereas higher-affinity antibodies induced later often use the same variable (V) genes that are somatically hypermutated. Clonal selection of B cells producing higher-affinity antibodies, known as affinity maturation, occurs in the specialized microenvironment of the germinal center (2–6).

Most conventional antibodies possess an antigen-binding site generated at the interface of the heavy- and light-chain V regions, and many groups have analyzed the effect of somatic mutation on binding specificity and the affinity of fragments derived from these antibodies. In some instances, the more flexible "induced fit" binding observed for germ-line clones was "fixed" in mutation-matured clones to give a "lock-and-key" mode of binding and, consequently, a higher binding affinity and specificity (7, 8). Other groups have shown that improvements in shape-complementarity with antigen are responsible for increasing affinity and specificity (9, 10). Much less research has focused on affinity maturation in ectothermic vertebrates. Furthermore, little is known of how single-domain antibody fragments, which lack one of the V domains, are matured. A study of an anti-hen egg-white lysozyme (HEL) camel heavy-chain antibody variable (VHH) domain in its germ line and mutated form showed that, despite the lack of binding-site plasticity conferred by pairing with a second domain and the presence of a complementarity-determining region (CDR)3-constraining disulphide bond, a 300-fold increase in binding affinity was achieved by increasing VHH-antigen complementarity and apolar buried surface area (11). However, all but one of the clones in the study were generated *in vitro* and, so, tell little of how the antigen-stimulated repertoire is generated.

The shark isotype IgNAR is a heavy-chain homodimer that, similarly, does not associate with light chain (12). Its V regions act as independent soluble units to bind antigen. IgNAR is a paucicopy (few-copy) gene family arranged in the cluster organization typical of elasmobranchs; of the four member genes, only two (type I and type II) are expressed in adult animals. Type I and type II V regions are highly similar in sequence but differ in the positions of their noncanonical Cys residues (13). The IgNAR V-region primary repertoire is entirely CDR3-based and is, subsequently, subject to high levels of apparent antigen-driven mutation (14). However, because the IgNAR V region utilizes three diversity (D) regions, requiring four rearrangement events, the primary repertoire contains clones with an unprecedented diversity of CDR3 length and amino acid composition (13, 15).

The crystal structures of both IgNAR V-region types (16, 17) have recently been solved. Surprisingly, the IgNAR V region is the only V domain that lacks a conventional CDR2. Instead, the IgNAR V region has a hypervariable loop that forms a belt around the middle of the molecule, as in a C1- (or S-) type domain. Because of its hypervariable yet unusual nature, we christened this loop hypervariable region (HV)2. The structures also revealed that the differential placement of noncanonical Cys residues induces very different CDR3 conformations in the two types, resulting in remarkably different binding-site topologies. Moreover, data from random (not antigen-selected) cDNA clones indicate that there is selection of mutations in the region of closest proximity to the CDR3 (i.e., HV2 of type I clones but CDR1 of type II) (15). Sequence analysis also revealed an additional HV between HV2 and CDR3 where mutations seemed to be under positive selection (14). After crystallographic analysis, this region was found to form the loop linking D and E strands in a region homologous to HV4 of T cell receptors (14, 18, 19). Because of its prominent location, structurally adjacent to CDR1, and its hypervariable nature, it is conceivable that HV4 may also participate in antigen binding.

Although most results indicate that affinity maturation in ectothermic vertebrates is poor (20, 21), two studies in nurse sharks found evidence that affinity maturation of monomeric IgM occurs after immunization (22, 23). It is thought that IgNAR (and monomeric IgM) production is a T-dependent response that provides the specificity of the shark humoral response (23), but, because of its apparent sensitivity to degradation *in vitro* (H.D. and M.F.F., unpublished work), affinity maturation of IgNAR has yet to be established.

Herein, we describe the generation of IgNAR V-region libraries from the immune tissues of a shark hyperimmunized to HEL. A

Conflict of interest statement: No conflicts declared.

This paper was submitted directly (Track II) to the PNAS office.

Abbreviations: CDR, complementarity-determining region; Fr, framework region; HEL, hen egg-white lysozyme; HV, hypervariable region; PBL, peripheral blood lymphocyte; V, variable.

Data deposition: All sequences reported in this paper have been deposited in the GenBank database (accession nos. DQ158874–DQ158892).

†To whom correspondence should be addressed. E-mail: hdooley@som.umaryland.edu.

www.pnas.org/cgi/doi/10.1073/pnas.0508341103

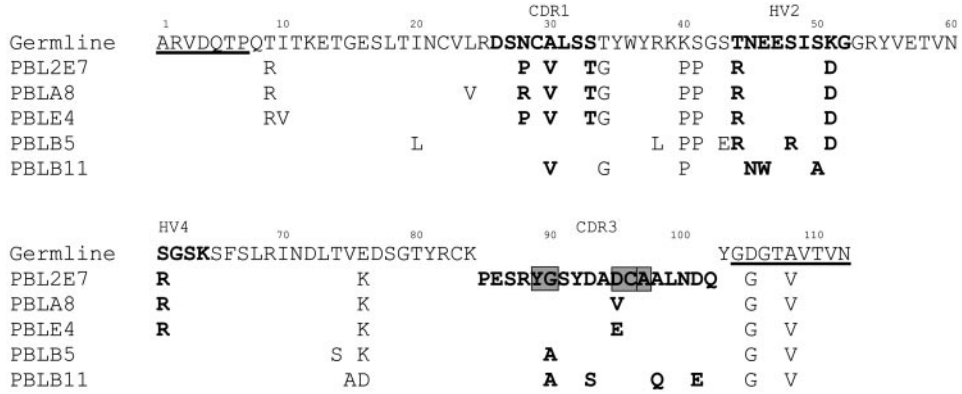

Fig. 1. Amino acid alignment for the five family clones against Fr1–Fr3 of their germ-line sequence. Numbers above the alignment indicate amino acid number, and underlining shows primer annealing sites. CDR1, HV2, HV4, and CDR3 are shown in bold. Residues in CDR3 contributed by D regions are indicated by shaded boxes.

family of antigen-binding type II clones was found that derived from the same ancestral clone but had been differentially mutated during *in vivo* expansion. The members of this family and a putative ancestral clone were studied with regard to their affinities and mutational status to try to better understand the role of this single-domain isotype *in vivo*. Surprisingly, the putative ancestral clone was found to bind antigen with nanomolar affinity. Nevertheless, through the introduction of somatic mutations, most of the family members analyzed had further improved their affinities, offering evidence not only that affinity maturation of the IgNAR isotype occurs but also demonstrating affinity maturation at the molecular level in ectotherms.

Results

Identification of the Type II Anti-HEL Family and Sequencing of Its Germ-Line Gene. Phage-displayed minilibraries of IgNAR V regions were generated from spleen, epigonal (the shark bone-marrow equivalent), and peripheral blood lymphocyte (PBL) tissues from the hyperimmunized animal and were subject to one round of low-stringency panning on HEL to maximize the diversity of binders selected. Of the 400 clones tested after panning, 15% were found to specifically bind HEL by ELISA. The vast majority of HEL-positive clones were obtained from the PBL minilibrary (≈24%), with fewer from epigonal (≈11%) and spleen (≈1%).

Eleven different sequences were found, of which five were found to be closely related (84–98% amino acid identity) and to contain a highly similar CDR3 region (Fig. 1). Because the IgNAR V region is generated by four rearrangement events (using 3 D regions), with associated addition and trimming, it is almost impossible that these clones were generated by independent rearrangement events. Indeed, during the sequencing of hundreds of clones picked at random from similar libraries (before selection), the same CDR3 was seldom encountered twice (ref. 14, and H.D. and M.F.F., unpublished work). Therefore, these clones are derived from the same ancestral clone but have been differentially mutated *in vivo* during expansion.

The family is derived from a type II clone, containing noncanonical Cys residues in CDR1 and CDR3 (Fig. 1). Sequencing of the germ-line genes from this animal enabled identification of the gene from which the family derived. All family members are highly mutated when compared with their germ-line sequence, containing 7–12 amino acid replacements in framework region (Fr)1–Fr3 (84 amino acids). Although the germ-line sequence encodes a high proportion of charged amino acids, some of the mutations observed introduce additional charged residues in place of uncharged ones. Thus, although solubility is encoded in the germ line, there seems to be an enhancement of this feature after mutation. The substitutions T9R and T44R exemplify this enhancement, both being solvent-exposed residues distant from the binding region. A similar acquisition of acidic residues was observed in IgNAR V-region families discovered during sequencing of random cDNA clones (14); why this further solubilization should be favored is unknown but may be important under the high-salt (1,000 mosmol), high-urea (350 mM) conditions *in vivo* in sharks. The family CDR3, at 19 amino acids, is longer than average for type II clones (14). All three D regions were found in each of the clones and the noncanonical Cys residue in CDR3 is encoded by D2 from its preferred reading frame (Fig. 1) (13). The CDR3 of the family also contained a number of charged amino acids that are under-represented in conventional antibody HCDR3s (24, 25). CDR3 also contains two tyrosine residues, which, through their ring structure and hydroxyl R group, usually increase the surface area available for antigen interaction and hydrophilicity (26). The Tyr-92 codon carries synonymous mutations, indicating negative selection on this residue in the HEL-binding clones, thus suggesting that T92 plays an important role in antigen interaction. Synonymous mutations were also observed in other residues known to be vital to IgNAR V-region structure: Gly-52 (in the turn from HV2 into Fr3) Arg-82 (increases solubility), Cys-83, and Cys-96 (disulfide bonding) (indicated in bold in Fig. 5, which is published as supporting information on the PNAS web site).

Amplification of Additional Type II Family Members. Because of the cluster organization and paucicopy nature of IgNAR, we thought that by targeting this rearrangement event, we could find other clones in this family. A D3-J region boundary-specific primer (A8JCDR3) was designed and used for RT-PCR on epigonal, spleen, and PBL RNA, resulting in amplification of 10 previously unidentified members (Fig. 2). Some of the initial family members (isolated through binding) were found a second time by RT-PCR, and many clones were amplified from multiple tissues, giving us confidence that our PCR strategy was working as expected. Mirroring the antigen-binding results, more family clones were isolated by RT-PCR from PBL ($n = 10$) and epigonal ($n = 9$) than from spleen ($n = 3$).

In general, the extended-family clones fall roughly into two groups; the first group (encompassing clones Epi6, Epi7, Epi8, Epi10, Epi13, and Epi14) appeared to have undergone one round of mutation, targeted mainly to CDR1-Fr2. The second group (PBLA8 and all remaining clones) were more highly mutated, with replacements in both CDR1-Fr2 and HV2. The clone PBLB5, with mutations in HV2 but not CDR1, does not conform to the mutation pattern observed for the other family members (Figs. 2 and 5). Especially noticeable is the presence of germ-line residues A30 and

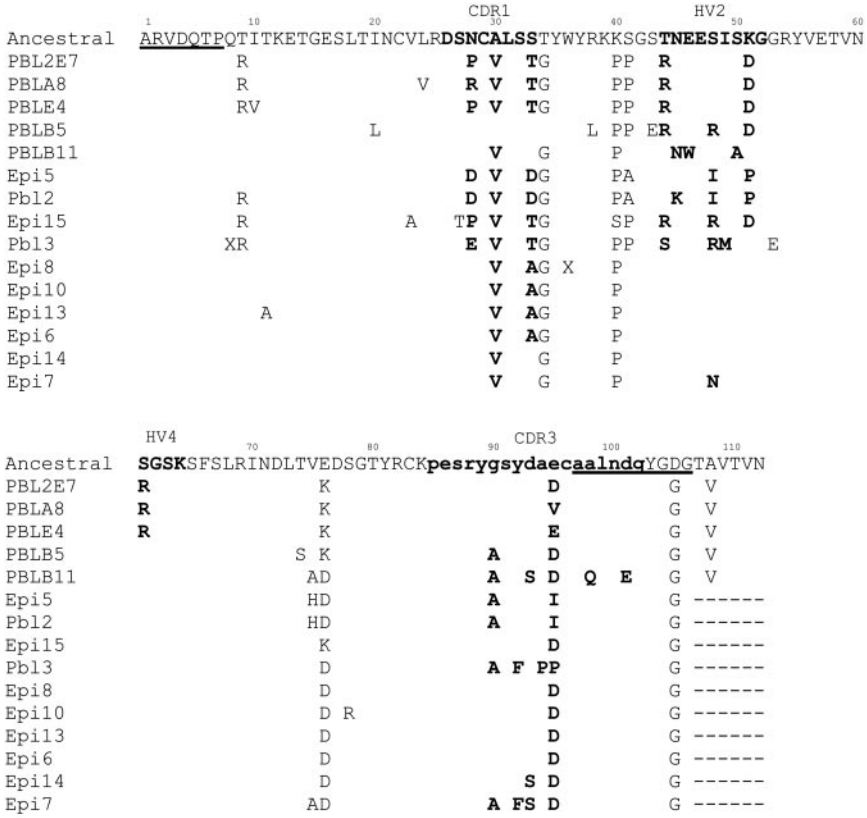

Fig. 2. Amino acid alignment for the extended family clones against that of the putative ancestral clone. Numbers above the alignment indicate the amino acid number, and underlining indicates primer annealing sites. CDR1, HV2, HV4, and CDR3 are shown in bold.

T34, which are mutated to V30 and G34 in all the other family clones and, so, probably arose early in family phylogeny. Analysis of the nucleotide alignment (Fig. 5) indicates that PBLB5 is either derived from a gene-conversion event or (more likely) is a PCR chimera that arose during library construction and is derived from the Fr1-Fr2 of a (differently mutated) nonfamily clone fused to the Fr2-Fr4 of the family (with the actual swap probably occurring around amino acid 39). Despite its probable origin as a PCR chimera, we decided to include PBLB5 in the analysis because of its usefulness for determining the role of CDR1 mutations in improving affinity.

The type II germ line from which the family is derived encodes 11 conventional mutation hotspot motifs (RGYW or WRCY), distributed throughout the domain but with a slight clustering in and around CDR1 (see Fig. 6, which is published as supporting information on the PNAS web site). An additional 4–5 hotspots are encoded within the CDR3 of the family clones. A Wu–Kabat plot was drawn to examine family variability in the context of mutation hotspots (see Fig. 7, which is published as supporting information on the PNAS web site). Half the positions identified as highly variable (scores >4) are located at mutational hotspots ($n = 5$ of 10), whereas the other positions had been identified by Diaz *et al.* (27) as nonconventional hotpots; amino acids 40–41 and 44–45 are encoded by runs of adenines, which are prone to mutation, presumably as a consequence of polymerase slippage; position 51 falls within a hairpin loop generated by a palindrome across Fr2/HV2. Many mutations were tandem in nature (nontemplated mutation of tandem bases), a mutational pattern specific to shark Ig genes (14, 28). Not all mutational hotspots gave rise to positions that were highly variable; for instance, of the hotspots identified within CDR3, only one has a variability >4. Antigen-binding is generally CDR3-dependent; mutations in this region could disrupt the binding site, resulting in counterselection *in vivo*. The highly variable residue in CDR3 is adjacent to the noncanonical Cys, which forms the constraining disulfide bond with that of CDR1. Thus, this residue is unlikely to be involved in antigen binding and be more "permissive" as to which amino acids may be tolerated in this position. In two members of the extended family (PBL3 and Epi7), the Tyr-92 residue postulated to have a role in antigen binding was mutated to Phe. Further study of these clones would tell whether the tyrosine-specific hydroxyl group is vital to antigen binding.

We instigated this PCR-based approach in the hope of finding less-mutated family clones, enabling us to study the order of mutation introduction and its effect on binding affinity. However, all of the clones found were too highly mutated to enable the analysis we desired. Because RNA had been prepared from PBLs taken just as this shark showed an increase in HEL-specific IgNAR (23), we tried to amplify family members from these samples instead. Repeated attempts at RT-PCR amplification of family members with the primer A8JCDR3 (anneals to D3-J of PBLA8) and a second primer A8JCDR3-long (anneals to D2-D3-J) failed to isolate additional family members. A number of nested RT-PCR approaches were also attempted, with little success. From the clones obtained, we saw other (nonfamily) V regions that used the same D3-J rearrangement but different V-D1 and D1-D2. Thus, family clones were either not present in the peripheral blood at this point in the immunization course or were too few to amplify.

Ancestral Clone Reconstruction. Because we were unsuccessful in finding less-mutated family clones by PCR, a putative "ancestral clone" was constructed, based on the type II germ-line sequence. The Fr1–Fr3 region of the genomic clone was PCR amplified and a family CDR3-Fr4 grafted onto this fragment by successive rounds of PCR extension. The strategy worked well, and a clone was

Table 1. Biacore data for the selected family clones

Clone	K_a (1/Ms)	K_d (1/s)	K_D (nM)
PBLA8	0.9×10^5	1.0×10^{-4}	1.0 (0.2)
PBLB11	3.0×10^5	1.4×10^{-3}	5.0 (1.6)
Epi6	2.1×10^5	1.6×10^{-3}	8.5 (4.8)
Ancestral	2.1×10^5	2.0×10^{-3}	9.5 (0)
PBLB5	0.5×10^5	1.5×10^{-3}	30 (8.5)

Affinity constants (K_D) were calculated as association constant (K_a) over dissociation constant (K_d), and the mean for each was calculated; SDs are indicated in parentheses. Data are the means of two to three experimental repeats with duplicate runs per experiment.

produced that represents the putative (unmutated) ancestral clone (Fig. 2).

Determination of Specificity and Affinity. Affinity-purified protein was produced for the original family members, Epi6, and the ancestral clone. All clones were checked for antigen binding by ELISA (data not shown) and selected clones subjected to analysis by BIAcore (Uppsala, Sweden). Of the clones chosen for analysis, PBLA8 was selected as an example of a clone with both CDR1 and HV2 mutations. It was not surprising that the "highly similar" clones PBLA8, PBL2E7, and PBLE4 all bound equally by ELISA. Clones PBLB11 and Epi6 were chosen for their unique HV2 mutation pattern and lack of HV2 mutation, respectively. Despite its probable origin as a PCR artifact, we decided to include PBLB5 as a fortuitous example of a clone mutated in HV2 but not CDR1 to gauge the effect of CDR1 mutation on binding. The real-time kinetics data obtained are shown in Table 1. The affinity of the putative ancestral clone was much higher (nM) than we had expected for an unmutated clone. However, we have reported a similarly high affinity for another HEL-binding IgNAR V region that had only a single amino acid replacement compared with its germ line (29). The 10-fold increase in affinity observed for PBLA8 when compared with ancestral is mainly a consequence of a slower dissociation rate (≈5-fold slower than ancestral), whereas the association rate is only fractionally improved (≈2-fold).

To generate the secondary repertoire, IgNAR V genes mutate extensively in an antigen-driven manner (14). From randomly sequenced clones, it was noted that type II clones showed selection of mutations in CDR1 (15). The very similar affinities of ancestral and Epi6 clones seem to indicate that the presence mutations in HV2 has little influence on antigen binding. In contrast, the lower (comparative) affinity of PBLB5 seems to indicate that mutations in CDR1 are important in modulating antigen binding. It is unlikely that the drop in affinity shown by PBLB5 is because of steric hindrance at the antigen–antibody interface, because all the mutations in this clone map away from the top of the molecule. Rather, it may be that one or more changes alter the take-off angle or flexibility of a CDR-bearing loop in a way that hinders antigen binding.

Structural Analysis. Because we had generated a model for the type II IgNAR V region (in ref. 16, confirmed by ref. 17) it was possible to map the position of various changes to gain insight into how, or whether, the changes influence binding. Mapping of changes between PBLA8, which had the highest affinity and most amino acid replacements, and ancestral clone sequences showed that most mutations mapped to the top of the molecule around the CDR3/1 border. Very few mutations were found in the vicinity of HV2, but (curiously) there was a cluster of mutations at the very bottom of the molecule (Fig. 3). The PBLA8-specific S61R substitution was mapped to the tip of the HV4 region (16), the hypervariable loop structurally adjacent to CDR1 (Fig. 4). We thought that this residue was ideally placed to influence antigen binding and that it may be partly responsible for the higher affinity of PBLA8. In a similar

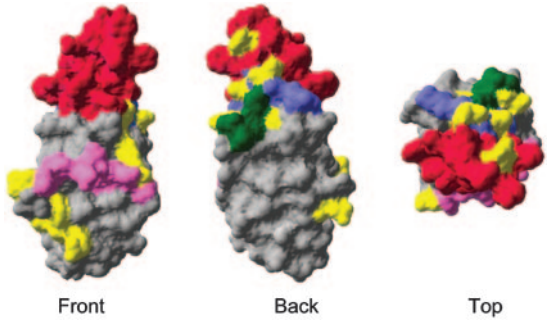

Fig. 3. Type II V-region model, mapping the position of amino acid changes between clone PBLA8 and the putative ancestral clone. CDR1 is shown in blue, HV2 in magenta, HV4 in green, CDR3 in red, and mutated residues in yellow.

comparison of Epi6 and the ancestral clone, most of the changes were, again, located in or around the CDR3/1 region at the apex of the molecule (data not shown). Immediately apparent was the interesting position of the CDR1 change A30V, adjacent to CDR3 at the top of the molecule (Fig. 4), in an ideal position to influence antigen binding. Again the "front" of the molecule, across which HV2 runs, showed very few mutations, but the cluster of mutations at the bottom of the molecule was once again apparent.

Ancestral Clone with A30V or S61R Substitutions. As described above, the two mutations A30V in CDR1 and S61R in HV4 could contribute to the increase in affinity between the ancestral clone and PBLA8. Although Gly-34 and Pro-40, present in all family clones, were also initially considered for analysis, they were discarded when they were mapped to the bottom of the domain, distant from the binding site. Another candidate, N28R, which, like A30V, lies within CDR1 at the top of the molecule, was thought unlikely to be influencing affinity, because this residue is mutated to proline in clones PBL2E7 and PBLE4, which bind by ELISA with exactly the same profile as PBLA8.

To test our hypothesis, we generated ancestral clones carrying either the A30V or S61R mutations alone and analyzed the affinity

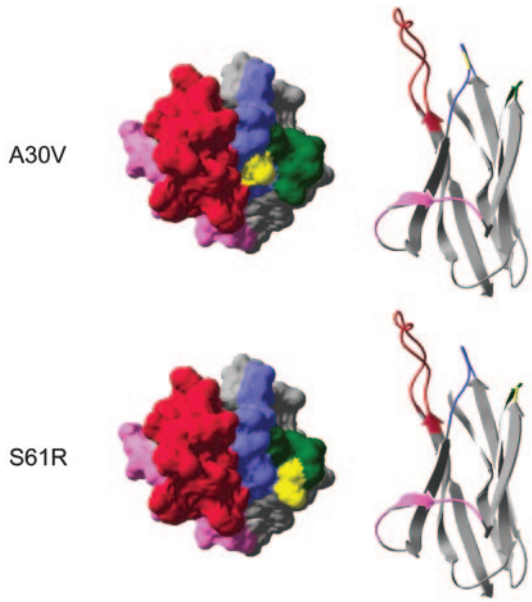

Fig. 4. Type II V-region model mapping the position of amino acid changes A30V and S61R, which were postulated to be important in improving affinity for antigen. CDR1 is shown in blue, HV2 in magenta, HV4 in green, CDR3 in red, and mutated residues in yellow.

Table 2. Biacore data for the ancestral mutants A30V and S61R

Clone	K_a (1/Ms)	K_d (1/s)	K_D (nM)
Ancestral	2.1×10^5	2.0×10^{-3}	9.5 (0)
A30V	1.4×10^5	1.6×10^{-3}	10 (1.3)
S61R	3.5×10^5	1.2×10^{-3}	3.3 (0.07)

Affinity constant (K_D) is calculated as for data in Table 1. SDs are indicated in parentheses.

of the mutants (Table 2). Kinetic data showed that the A30V substitution did not contribute to the increase in affinity, despite the close spatial proximity of CDRs 1 and 3. Conversely, the introduction of the S61R mutation into the ancestral clone improved affinity for antigen 3-fold, equally contributed by small (≈1.5-fold) increases in both association and dissociation rates. These data prove that the HV4 region can also be involved in antigen binding in the IgNAR V region. However, the affinity of this mutant is still 3-fold lower than that of PBLA8, indicating the presence of other unidentified mutations that also contribute to affinity improvement by further slowing the dissociation rate.

Discussion

The canonical model of affinity maturation is that of a fine-tuning process. Antibodies are formed from unmodified germ-line segments; thus, the pool from which antigen-binders can be selected is limited by the number of these segments in the genome and how efficiently they are rearranged. In most organisms, this germ-line-encoded diversity is complemented by rounds of somatic hypermutation and selection to incrementally improve the binding specificities selected from the primary repertoire. However, the degree to which different organisms rely on the fine-tuning conferred through somatic hypermutation appears to somewhat of a "sliding scale." According to recent publications, the camel single-domain VHH repertoire seems structurally limited (30), so low- (μM) affinity binders are selected from the primary repertoire, and mutation is required to significantly (1,000-fold) improve binding affinity (11). In contrast, the study of an IgNAR V-region family presented here demonstrated that high-affinity (nM) binders could be selected directly from the primary repertoire. The presence of these high-affinity binders is probably a consequence of the huge structural diversity imparted through the rearrangement of three D regions (the likes of which is not found in any other shark or nonshark Ig isotype) and the different CDR3 conformations forced by differential disulfide bonding in the two V-region types (13, 15). After the *in vivo* introduction of somatic mutations, we see incremental increases in affinity, strongly indicative of affinity maturation, but these improvements are comparatively small (≈10-fold). All evidence to date indicates that sharks do not have (conventional) germinal centers (31). However, because the frequency of mutation of IgNAR is known to be very high, in some instances exceeding that of mammalian Igs, it may be that it is the selection of mutants that is suboptimal. The generation of such an extensive primary repertoire in sharks may be compensatory for the absence of the strongly selective environment of the germinal center.

Analysis of random cDNA clones showed differential selection of mutations in HV2 and CDR1 (15), indicating that they could contribute to antigen binding with CDR3; this finding was subsequently confirmed for CDR1 through structural analysis of a type I clone (16) and for CDR3 by *in vitro* mutation of a type II clone (32). Because of a similar selection of mutations, combined with its position neighboring CDR1, the loop designated as HV4 might also modulate antigen binding (14, 27). In this study, the introduction of the mutation S61R, mapped to the tip of HV4, into the ancestral background was able to improve affinity 3-fold. The IgNAR V region, consequently, has a total of four hypervariable regions (CDR1, CDR3, and HV4 at the top and HV2 on the front of the domain) that it can use, in various combinations, to generate an enormous surface over which antigen-binding can occur. As more structures for this single domain are solved, we hope to uncover how much of the potential binding surface is actually used *in vivo*.

It was clear during the analysis of the family clones that some clones carried a high number of mutations which, because of their location, were unlikely to participate in antigen binding. A similar observation has been made in studies of affinity-matured antibodies from mammalian species (33). This high load of mutations is likely the result of repeated cycles of somatic mutation and indicates that mutations that do not adversely affect antigen binding will be tolerated. Indeed, during analysis of extended-family members, we thought there had been a stepwise acquisition of mutations, with some clones seeming to have undergone a single cycle of mutation and others at least two cycles. The first round of selection seems to have been targeted to CDR1, and many of these mutations appear to be under selection. The selection of mutations in CDR1 is almost certainly a consequence of its role in antigen-binding in this family. It is also apparent that the replacements in CDR1 are the result of only a few (three or four?) mutational events, some of which introduce tandem mutations (Fig. 5). The next round(s) of mutation are targeted to HV2 (which, in this family, is not involved in antigen binding) and, therefore, are under less selection (positive or negative) than those in CDR1. As an aside, it would seem that the introduction of tandem mutations may be used by sharks to achieve their extremely high mutation rate; animals with slow rates of B cell replication would undergo fewer rounds of replication in a set time than those with a high rate of replication. Thus, to attain a sufficient rate of mutation, shark B cells may need to introduce more mutations per round of replication by changing multiple bases in a single mutational event.

As mentioned, during a previous study of random cDNA clones derived from amplification of secretory IgNAR, three similar V-region families were identified (14), allowing analysis of mutation acquisition; however, because the stimulating antigen was unknown, the role of these mutations in affinity maturation could not be studied. In addition, after the selection of a different library for binders to an unrelated protein antigen, we isolated two more (smaller) families. The ability to easily isolate such families of clones seems to be specific to IgNAR V regions, possibly because of a combination of its cluster organization, paucicopy nature, and extensive primary repertoire. In the discovery of such families, combined with the single-domain nature of the V region (lacking a second domain, which complicates analysis), we appear to have fortuitously stumbled on an ideal system for studying somatic hypermutation in the context of antigen binding.

Materials and Methods

Sequencing of Unrearranged, Germ-Line IgNAR V Regions. Genomic DNA was isolated from erythrocytes of the immunized animal. PCR amplification of the unrearranged IgNAR V regions was conducted by using 250 ng of DNA and the IgNAR V-region primers NAR F4For1, NAR F4For2, and NAR Fr1Rev (29). PCR products were cloned into pCR-2.1 by using the TA-cloning system (Invitrogen) and insert-positive clones identified for sequencing by blue/white selection.

Minilibrary Construction and Clone Isolation. To induce an anti-HEL response, an adult nurse shark was immunized once with 20 mg of HEL in complete Freunds adjuvant s.c. in the lateral fin. Four s.c. boosts of 20 mg of HEL in incomplete Freunds adjuvant were given over the subsequent 7 months. Additional boosts of 250 μg of soluble HEL were given i.v. at 10 and 24 months (1 month before killing) to ensure a high titer of antigen-specific antibody (23). Total RNA was prepared from PBLs, epigonal, or spleen. RNA from each tissue was used separately at 1 μg/μl as template for IgNAR V-region amplification and minilibrary construction (each of ≈5×10^4 members) (29). A single round of nonstringent panning was

undertaken for each minilibrary by incubating 1 ml of phage in 3 ml of 2% casein solution in HEL-coated (100 μg/ml) and casein-blocked maxisorp immunotubes for 2 h. Before elution, the immunotubes were washed 10 times with PBS to remove nonspecifically bound phage. Phage were rescued as detailed in ref. 29. Clones were tested by ELISA for binding by using monoclonal phage supernatant. Binding was detected with anti-M13 horseradish peroxidase-conjugated monoclonal antibody (Amersham Pharmacia Biotech). Plasmid was prepared from HEL-positive clones and their inserts sequenced.

Amplification of Additional Type II Family Members. Additional family members were amplified from RNA for each tissue by using the D3-J region-specific primer A8JCDR3 (5′-GCC ACC TCC GTA CTG GTC ATT AAG CGC AGC-3′) and the Fr1 primer NAR Fr1Rev (29). The PCR product of ≈350 bp was cloned into pCR-2.1 and insert-positive clones identified for sequencing as above. For samples where no clones were obtained with A8JCDR3, a longer primer, A8JCDR3 long (5′-GTC ATT AAG CGC AGC ACA CTC AGC ATC GTA CGA TCC ATA TCG-3′), was designed that anneals through D2-J of the family CDR3.

Reconstruction of Epi6. Clone Epi6 was PCR-amplified from TA vector with the primers NAR Fr1Rev and NAR F4For2 to graft the Fr4 region back onto the end of the clone.

Ancestral Clone Reconstruction. Plasmid was prepared for the genomic clone containing the unrearranged V-region sequence from which the type II family is derived. The CDR3-Fr4 of the family clone PBLE4 was grafted onto the corresponding germ-line Fr1–Fr3 by overlapping PCR extension. Four rounds of PCR were used to reconstruct the CDR3, each primer being used with the NAR Fr1Rev primer (as above). Extension primers used were as follows: round 1, H29 extend (5′-CGA AGC ATA TCG GCT TTC GGG CTT GCA TCG ATA CGA-3′); round 2, A8JCDR3 long; round 3, A8JCDR3; and round 4, NAR Fr4For2 (as above).

Generation of Ancestral A30V and S61R Mutants. Nucleotide sequences encoding the germ-line gene but incorporating the mutations A30V (GCA to GTA) or S61R (AGC to CGT) and flanked by NcoI and NotI restriction enzyme sites to aid cloning into pIMSΔHuCκ were synthesized commercially (www.blueheronbio.com).

Protein Expression and Purification. For expression, V regions were cloned into the vector pIMSΔHuCκ through their NcoI and NotI restriction enzyme sites. Upon induction with IPTG, this vector produces soluble protein tagged with a hexa-histidine tail. Protein was harvested from the periplasmic fraction (method detailed in ref. 34 but omitting lysozyme from the fractionation buffer) and purified by immobilized metal-affinity chromatography. Subsequent affinity-purification was performed by passage over a HEL-Sepharose column, eluting with 100 mM glycine·HCl, pH 2.8, and neutralizing with 1M Tris·HCl, pH 8. Protein was dialyzed against PBS and quantified by BCA assay. Concentrations were verified and purity established to be >95% by SDS/PAGE.

Determination of Affinity. Real-time interaction measurements were performed on a BIAcore 3000 biosensor (Amersham Pharmacia) as detailed in ref. 29. HEL-coating density on the CM5 chip was ≈265 resonance units (RU), and samples were run over this surface at a range of concentrations between 200 and 0.75 nM. RUs for the control surface (activated and blocked with ethanolamine) were removed before analysis and the resultant sensorgrams analyzed with the program BIAEVALUATION 3.2.

Molecular Modeling. The IgNAR Type II domain was modeled on the Type I structure, with the CDR3 region based on that of the camel VHH domain AMD10 (detailed in ref. 16).

We thank James Walsh and the staff of the National Aquarium in Baltimore for their meticulous care of our sharks and Drs. Jan Cerny, Louis Du Pasquier, and Marilyn Diaz for invaluable comments during the drafting of this manuscript. This work was supported, in part, by National Institutes of Health Grant RR06603 (to H.D. and M.F.F.).

1. Eisen, H. N. & Siskind, G. W. (1964) *Biochemistry* **155,** 996–1008.
2. Griffiths, G. M., Berek, C., Kaartinen, M. & Milstein, C. (1984) *Nature* **312,** 271–275.
3. Berek, C., Griffiths, G. M. & Milstein, C. (1985) *Nature* **316,** 412–418.
4. Berek, C., Berger, A. & Apel, M. (1991) *Cell* **67,** 1121–1129.
5. Ziegner, M., Steinhauser, G. & Berek, C. (1994) *Eur. J. Immunol.* **24,** 2393–2400.
6. Ziegner, M. & Berek, C. (1994) *Adv. Exp. Med. Biol.* **355,** 201–205.
7. Wedemayer, G. J., Patten, P. A., Wang, L. H., Schultz, P. G. & Stevens, R. C. (1997) *Science* **276,** 1665–1669.
8. Yin, J., Beuscher, A. E., Andryski, S. E., Stevens, R. C. & Schultz, P. G. (2003) *J. Mol. Biol.* **330,** 651–656.
9. Li, Y., Li, H., Yang, F., Smith-Gill, S. J. & Mariuzza, R. A. (2003) *Nat. Struct. Biol.* **10,** 482–488.
10. Cauerhff, A., Goldbaum, F. A. & Braden, B. C. (2004) *Proc. Natl. Acad. Sci. USA* **101,** 3539–3544.
11. De Genst, E., Handelberg, F., Van, M. A., Vynck, S., Loris, R., Wyns, L. & Muyldermans, S. (2004) *J. Biol. Chem.* **279,** 53593–53601.
12. Greenberg, A. S., Avila, D., Hughes, M., Hughes, A., McKinney, E. C. & Flajnik, M. F. (1995) *Nature* **374,** 168–173.
13. Roux, K. H., Greenberg, A. S., Greene, L., Strelets, L., Avila, D., McKinney, E. C. & Flajnik, M. F. (1998) *Proc. Natl. Acad. Sci. USA* **95,** 11804–11809.
14. Diaz, M., Greenberg, A. S. & Flajnik, M. F. (1998) *Proc. Natl. Acad. Sci. USA* **95,** 14343–14348.
15. Diaz, M., Stanfield, R. L., Greenberg, A. S. & Flajnik, M. F. (2002) *Immunogenetics* **54,** 501–512.
16. Stanfield, R. L., Dooley, H., Flajnik, M. F. & Wilson, I. A. (2004) *Science* **305,** 1770–1773.
17. Streltsov, V. A., Varghese, J. N., Carmichael, J. A., Irving, R. A., Hudson, P. J. & Nuttall, S. D. (2004) *Proc. Natl. Acad. Sci. USA* **101,** 12444–12449.
18. Patten, P., Yokota, T., Rothbard, J., Chien, Y., Arai, K. & Davis, M. M. (1984) *Nature* **312,** 40–46.
19. Garcia, K. C., Degano, M., Pease, L. R., Huang, M., Peterson, P. A., Teyton, L. & Wilson, I. A. (1998) *Science* **279,** 1166–1172.
20. Hsu, E. (1998) *Immunol. Rev.* **162,** 25–36.
21. Du Pasquier, L., Wilson, M., Greenberg, A. S. & Flajnik, M. F. (1998) *Curr. Top. Microbiol. Immunol.* **229,** 199–216.
22. Voss, E. W., Jr., & Sigel, M. M. (1972) *J. Immunol.* **109,** 665–673.
23. Dooley, H. & Flajnik, M. F. (2005) *Eur. J. Immunol.* **35,** 936–945.
24. Collis, A. V., Brouwer, A. P. & Martin, A. C. (2003) *J. Mol. Biol.* **325,** 337–354.
25. Ivanov, I., Link, J., Ippolito, G. C. & Schroeder, H. W., Jr. (2002) in *The Antibodies* 7, eds. Zanetti, M. & Capra, J. D. (Taylor & Francis, London), pp. 43–67.
26. Mian, I. S., Bradwell, A. R. & Olson, A. J. (1991) *J. Mol. Biol.* **217,** 133–151.
27. Diaz, M., Velez, J., Singh, M., Cerny, J. & Flajnik, M. F. (1999) *Int. Immunol.* **11,** 825–833.
28. Lee, S. S., Tranchina, D., Ohta, Y., Flajnik, M. F. & Hsu, E. (2002) *Immunity* **16,** 571–582.
29. Dooley, H., Flajnik, M. F. & Porter, A. J. (2003) *Mol. Immunol.* **40,** 25–33.
30. De Genst, E., Silence, K., Ghahroudi, M. A., Decanniere, K., Loris, R., Kinne, J., Wyns, L. & Muyldermans, S. (2005) *J. Biol. Chem.* **280,** 14114–14121.
31. Zapata, A. & Amemiya, C. T. (2000) *Curr. Top. Microbiol. Immunol.* **248,** 67–107.
32. Nuttall, S. D., Humberstone, K. S., Krishnan, U. V., Carmichael, J. A., Doughty, L., Hattarki, M., Coley, A. M., Casey, J. L., Anders, R. F., Foley, M., *et al.* (2004) *Proteins* **55,** 187–197.
33. Alzari, P. M., Spinelli, S., Mariuzza, R. A., Boulot, G., Poljak, R. J., Jarvis, J. M. & Milstein, C. (1990) *EMBO J.* **9,** 3807–3814.
34. Dooley, H., Grant, S. D., Harris, W. J. & Porter, A. J. (1998) *Biotechnol. Appl. Biochem.* **28,** 77–83.